Journal of the European Ceramic Society **19** (1999) 119–123

PII: S0955-2219(98)00179-4
0955-2219/98/$—see front matter

Analysis of Near-Tip Crack Bridging in WC/Co Cermet

Giuseppe Pezzotti,[a]* Heinz Huebner,[b] Hiroyuki Suenobu,[a] Orfeo Sbaizero[c] and Toshihiko Nishida[a]

[a]Department of Materials, Kyoto Institute of Technology, Sakyo-ku, Matsugasaki, 606 Kyoto, Japan
[b]Department of Material Physics, Technical University of Hamburg-Harburg, D-21073 Hamburg, Germany
[c]Department of Materials Engineering, University of Trieste, 34127 Trieste, Italy

(Received 22 April 1998; accepted 20 July 1998)

Abstract

The remarkable toughening effect usually found in WC/Co cermets has been analyzed by means of a fracture mechanics approach based on R-*curve characterization and* in situ *measurements of crack opening displacement (COD). The use of a crack stabilizer specially designed for the bending geometry enabled to detect the rising* R-*curve behavior of the material starting from the very neighborhood behind the crack tip (i.e.* $< 100\,\mu m$*).* In situ *COD measurements were related to the rising* R-*curve behavior through theoretical equations for bridged cracks. As a result, the toughening effect in the cermet was explained using a constant (average) distribution of bridging stress which shields the crack in the very neighborhood behind its tip. The magnitude of the bridging stress was found to be close to the ultimate strength of the Co metal phase. Only a very minor effect on toughening was found to be operated by metal ligaments in regions far away from the crack tip.*

Keywords: composites, tungsten carbide, fracture, toughening, crack bridging

1 Introduction

Toughening of brittle matrices through the addition of a minor fraction of a ductile phase is a well recognized concept in the field of structural ceramics.[1] Accordingly, efforts have recently been directed towards the development of new processing routes to produce such cermet materials with higher efficiency.[2] Despite the improved processing ability, however, the theoretical directives for developing a cermet microstructure which can experience optimum toughness are not yet well clarified. From the experimental side, the presence of a metal phase with the morphology of a ductile binder, which continuously circumvents the ceramic grains, seems to be more effective than a discontinuous dispersion of metallic particles.[3] This assertion is mainly supported by the outcome of fracture mechanics analyses of the WC/Co cermet system, perhaps the toughest cermet material made so far available by traditional processing routes.[4] Recently, Kotoul[5] has presented a theoretical analysis of crack bridging process in the WC/Co system, with emphasis placed on the effect of the volume fraction of metal binder on fracture toughness. The main outcome of this analysis is that the cooperation of the cleavage process in the matrix grains and the tearing of binder ligaments results in a significant crack meandering, with the development of a bridging zone containing a high fraction of metal phase. In this paper, we have a, attempted to experimentally analyze the toughening behavior of the WC,/Co cermet by means of stable fracture experiments. In addition, scanning electron microscopy (SEM) observation and measurements of the crack opening displacement (COD), have been employed to quantitatively assess the typical extension of the bridging zone and the magnitude of the bridging stresses, which are provided by the metal ligaments in a process zone in the very neighborhood of the crack tip. The principal goal of this study has been that of quantifying the above two microscopic bridging parameters, which were theoretically discussed as inherent material properties in a previous paper.[6] The experimental evidences obtained by analysing the tough WC/Co system are thought to provide important research directives for the future development of new cermets with high toughness characteristics.

*To whom correspondence should be addressed.

2 Fracture Mechanics and Microscopy Experiments

The WC/Co material employed in this investigation was provided by Pozzo Co., International Saws (Udine, Italy) and contained a volume fraction of Co binder ~6wt%. The average grain size of the WC matrix was 1·5 μm. Specimens for fracture mechanics testing were parallelepipeds 3×4×20 mm (B×W×L). A straight through notch with a relative length, a/W~0·5 was introduced at the center of the bars by a diamond cutter (blade thickness of 0·2 mm). For reducing the influence of the finite notch–tip radius on the monitored fracture behavior, the bottom part of the saw-notch was sharpened with a razor blade sprinkled with fine diamond paste (1 μm). By this procedure, the notch root could be sharpened to a radius of $< 10\,\mu$m. In order to achieve stable, fracture propagation in bending geometry, a crack stabilizer[7] in three-point bending geometry was employed. This crack stabilizer allows to arrest the crack even after very short extensions (i.e., of few tens micron order), thus enabling the determination of very near-tip rising *R*-curve behaviors. The span of the loading jig was 16 mm. The load-displacement relation was directly measured with semiconductor strain gauges placed both on the loading bar and on the tensile surface of the specimen. Further details of the notching procedure and the bending stabilizer have been reported elsewhere.[8,9] *R*-curve data were collected from the load–displacement curves obtained under the relatively fast cross-head speed of 0·1 mm/min^{-1}. The crack length was measured by SEM during successive steps of the stable crack propagation, concurrently with collecting a COD map along the crack path. The SEM apparatus was an Hitachi S-800, using a field emission gun operating at 30 kV. The procedure for measuring COD on the crack profile was the same as that suggested by Rödel *et al.*[10] The crack resistance value, K_R, relative to the actual crack extension was calculated from standard equations for three-point bending geometry.

3 Results and Discussion

Figure 1 shows a typical load (P) versus displacement (u) curve experienced by the WC/Co cermet during stable fracture propagation in bending. in the inset of Fig. 1, also the dependence of the crack Resistance K_p on the crack length, Δa, measured from the notch root is shown, the latter parameter being determined by SEM observations on the crack profile during stable propagation. These data clearly prove that the rising *R*-curve behavior of

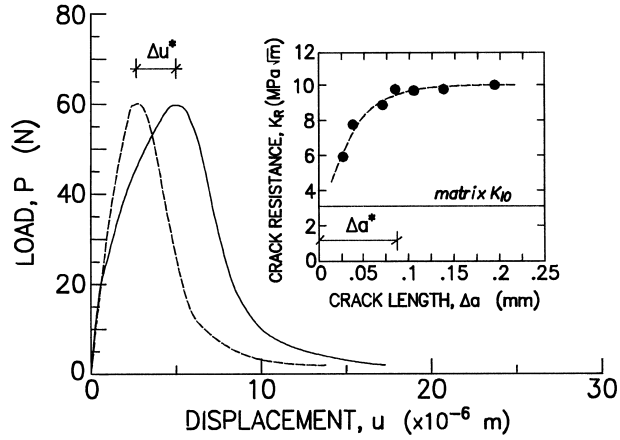

Fig. 1. Experimental P–u relation determined by stable crack propagation in bending (full line) in comparison with the theoretical P–u dependence predicted for linearly elastic material (broken line). The rising *R*-curve behavior, as determined by stable fracture experiments, is shown in the inset.

the WC/Co material abruptly takes place within a rather short crack extension (i.e. $\Delta a = 80 \div 100\,\mu$m) up to a plateau value $(K_R)_{max} \sim 10$ MPa×m$^{1/2}$ (i.e. the crack resistance value calculated at the maximum load, P_C). The work of fracture, Γ, was calculated from the area under the P versus u plot, by dividing it by twice the fractured surface area. The Γ value calculated from averaging three data of different tests was 95·6 J m^{-2}. This value is some what larger than the work of fracture reported by Engel and Huebner[11] (i.e. ~70 J m^{-2}) for a WC/Co cermet with an average grain size of the WC grains ~0·76 μm. This difference may be due to the fact that the grain size of the present WC/Co cermet material is nearly double than that tested by Engel and Huebner. An interesting feature of the P versus u plot is that, upon initial loading, the curve loses its linearity at a relatively low P value, namely at $P/P_C \sim 1/3$. This load corresponds to the critical stress intensity for crack propagation in the brittle WC matrix, namely, $K_{I0} = 3{\cdot}2$ MPa×m$^{1/2}$. The detected change in specimen compliance during initial loading reflects the occurrence of a (subcritical) crack propagation from the tip of the notch prior to achieving the maximum load P_C. A confirmation of this compliance results could be obtained by SEM observation of the neighborhood of a notch root in a specimen loaded up to $P/P_C = 0{\cdot}5$. In Fig. 2, cleaved WC grains are shown which failed ahead of the notch under a load below the critical value, P_C, for stable crack propagation. The P versus u plot of the WC/Co cermet specimen can be theoretically predicted when the process-zone behind the crack tip (i.e. the crack extension along which toughening mechanisms are activated) can be considered to be small as compared with the total crack length. This is the case in which the bridging mechanism can be considered to contribute

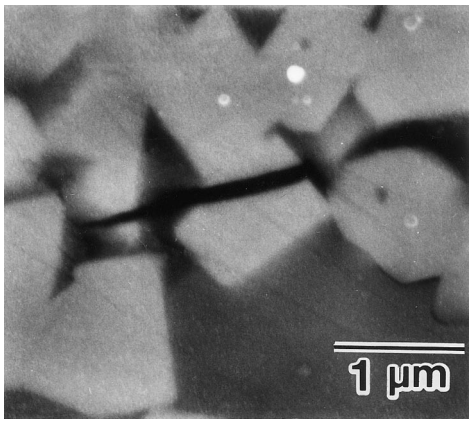

Fig. 2. Cleaved WC matrix grains observed by SEM ahead of the notch tip upon loading below the critical load for crack propagation (i.e. $P/P_C \approx 0{\cdot}5$).

to the intrinsic toughness of the material. Provided that the elastic constants (i.e. the Young's modulus, E, and the Poisson's ratio, ν) of the material and the notch depth are known, the theoretical load-displacement curve of a linearly elastic material can be determined, according to the analytical procedure given by Srawley and Gross.[12] The result of this calculation is shown by a dashed line in Fig. 1. Such a theoretical P–u curve represents the compliance response of a brittle material to a constant critical stress intensity factor, $K_{IC} = (K_R)_{max}$, (i.e. independent of the crack length).

Leaving aside the change in compliance associated with the subcritical crack extension (indicated as Δu^* in Fig. 1) in the WC matrix, the experimental P–u curve shows a morphology almost coincident with the theoretical compliance. Particularly, the load decrease upon crack extension occurs in nearly the same way as in a linearly elastic material. This characteristic of the P–u curve means that, in the present WC/Co material, the crack bridging mechanism can only be exploited within a very short process zone behind the crack tip, while no toughening mechanism is operative in the long-range crack extension. Using standard equations to relate the change in compliance, Δu^*, to the crack length[11] leads to assess a (subcritical) crack extension $\Delta a^* = 120\,\mu$m, in good agreement with the Δa^* value experimentally found from the K_R versus Δa plot (cf. Figure 1). The nearly linear elastic behavior found by the present fracture toughness analysis is in agreement with the outcome of an analysis of strength behavior previously reported for WC/Co cermet.[12]

Figure 3 shows a SEM picture of a portion of crack profile taken in the neighborhood behind the crack tip. Stretched Co ligaments are clearly visible, which are considered to provide the near-tip bridging effect in the present WC/Co material. SEM observations also revealed that such ligaments were broken in zones of the crack profile far away from the crack tip. Exploiting the good resolution of the field-emission SEM images, the construction of a COD map (cf. arrows in Fig. 3) was attempted for a crack extension $\Delta a = 100\,\mu$m behind the tip of a stably propagated crack. The results of this mapping experiment are summarized in Fig. 4(A). For comparison, the COD profile theoretically calculated for the WC matrix (i.e. in absence of bridging tractions) is also shown. The theoretical COD profile for an unbridged crack is given by the Irwin parabola.[13]

$$\delta_m(x) = [(K_R)_{max}/E'](8x/\pi)^{1/2} \tag{1}$$

On the other hand, the COD profile of a bridged crack is given as:[14]

$$\delta(x) = \delta_m(x) - (2/\pi E') \int_o^{\Delta a^*} \sigma_{BR}(x') \ln[|(x'^{1/2} + x^{1/2})/(x'^{1/2} - x^{1/2})|]\mathrm{d}x' \tag{2}$$

where x is the abscissa along the crack wake with origin at the crack tip, E' is the plain strain

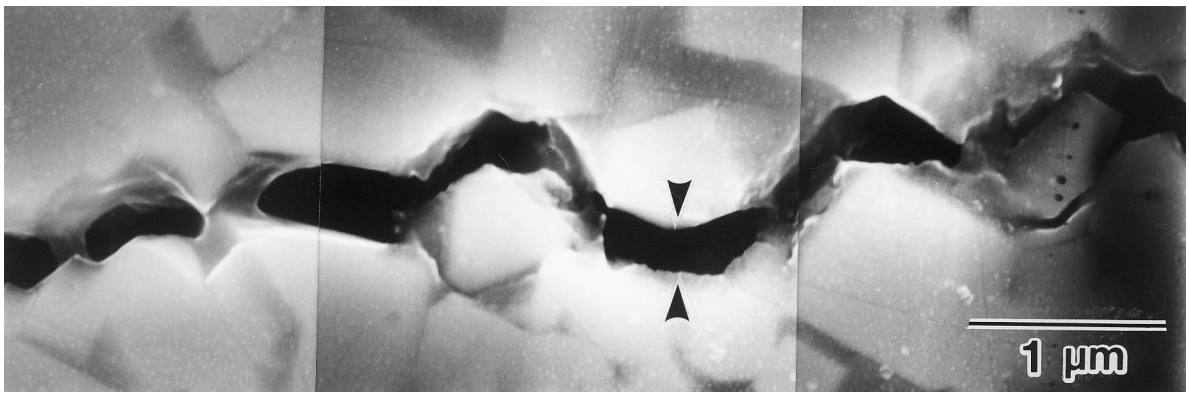

Fig. 3. SEM image of a portion of crack profile which was located $\approx 30\,\mu$m behind the crack tip under an applied $K_I = (K_R)_{max} \approx 10\text{MPa} \times \text{m}^{1/2}$. Stretched Co ligaments are clearly visible along the profile. The crack propagated from left to right. The arrows indicate an example of COD measurement, as performed throughout along the equilibrium crack.

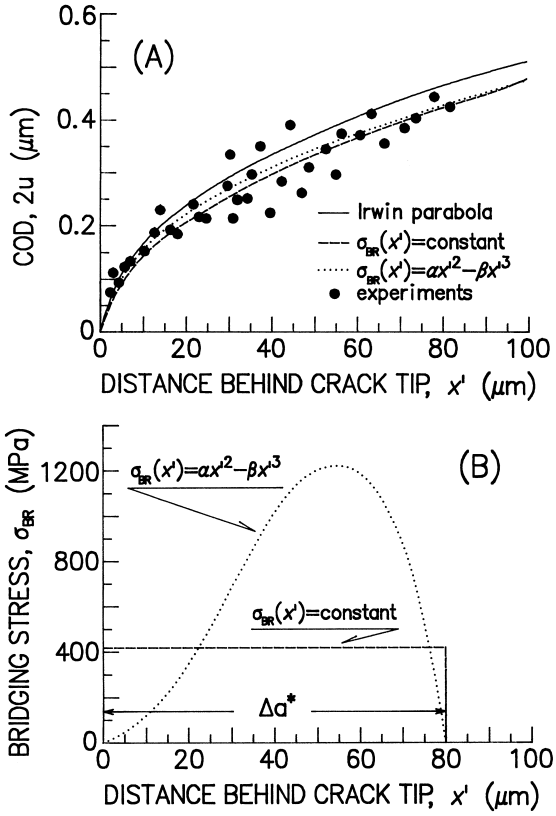

Fig. 4. (A) Experimental COD results from SEM mapping are compared with the Irwin COD parabola [cf. eqn (1)] for a linearly elastic material and the theoretical COD values calculated from the Barenblatt eqn (2). (B) Bridging stress distributions calculated from the experimental rising *R*-curve behavior of the WC/Co cermet. The calculation is performed both according to eqn (3) or by considering a constant bridging stress distribution, under the assumption of a bridging zone length, $\Delta a^* = 80\ \mu$m.

Young's modulus (i.e. measured as $E' = 620$ GPa in the present WC/Co cermet), σ_{BR} is the bridging stress and x' is the abscissa where such a stress is applied along the crack profile. In addition, the macroscopic *R*-curve behavior of the material can be related to the microscopic bridging stress function, $\sigma_{BR}(x')$, through the following equation:[15]

$$K_R = K_{I0} + (2/\pi)^{1/2} \int_o^{\Delta a} [\sigma_{BR}(x')/x'^{1/2}]\mathrm{d}x' \qquad (3)$$

The integral eqn (3) can be solved for the stress function $\sigma_{BR}(x')$ using the *R*-curve data, provided that a physically sound shape for the function $\sigma_{BR}(x')$ is chosen and the boundary conditions established. One possible choice for representing the bridging stress function is the functional form:

$$\sigma_{BR}(x') = \alpha'^2 - \beta x'^3 \qquad (4)$$

This function has been proposed and shown to be appropriate in a previous studies of nearby toughened ceramics.[16] In addition, a direct evaluation of near–tip bridging stresses in toughened Si_3N_4 ceramics by Raman microprobe spectroscopy[17] has also confirmed the validity of a functional stress form given in (4). A further choice can be that of considering a constant (average) stress field which shields the crack in the neighborhood of its tip. If the functional form in (4) is selected, after substituing in eqn (3) and integrating, the two arbitrary constants α and β can be determined from the K_R and K_{I0} data (cf. Fig. 1), by applying the boundary condition σ_{BR} for $x' = \Delta a^*$. In the case of constant bridging stress, the determination of the σ_{BR} value is straightforward from iterative integration of eqn (3). The results of this analytical procedure are shown in Fig. 4(A). For a bridging zone $\Delta a^* = 80\ \mu$m, the constants α and β were calculated as $1{\cdot}30\times10^{12}$ and $1{\cdot}63\times10^{16}$, respectively, when stresses and crack lengths are given in MPa and μm, respectively. The maximum bridging stress, $(\sigma_{BR})_{max}$ can be calculated by using the condition $\mathrm{d}\sigma_{BR}(x')/\mathrm{d}x' = 0$, which results in $(\sigma_{BR})_{max} = 4\alpha^3/(27\beta^2) = 1235$ MPa at $x' = 2\alpha/3\beta \approx 53\ \mu$m. When the bridging zone is taken as $\Delta a^* = 120\ \mu$m, the maximum stress value reduces to 1008 MPa, placed at $x' = 80\ \mu$m. A $(\sigma_{BR})_{max}$ of GPa order is however about twice the ultimate strength value reported for annealed Co metal.[8] Even assuming that a strong constraint effect exerted by the ceramic grains on the metal phase occurs,[19] it is difficult to justify such a high strength of the metal ligaments. In alternative, the very high maximum bridging stress may just be an artifact of the bridging stress distribution chosen. Closer to the actual strength reported for Co metal[18] is the value found by considering a constant bridging stress distribution, namely, $[\sigma_{BR}]_C = 420$ MPa. In order to discuss the validity of the two $\sigma_{BR}(x')$ functions, eqn (2) was numerically solved with using the bridging stress functions shown in Fig. 4(B). The COD functions calculated in this way are shown in Fig. 4(A) (cf. dotted line), in comparison with the Irwin COD parabola and the COD values experimentally determined by SEM observations. The Irwin parabola for the unbridged crack lies well above the experimental COD data. On the other hand, theoretical results obtained by a constant stress distribution $[\sigma_{BR}]_C = 420$ MPa seem to fit the experimental COD results with a better agreement as compared to the function in (4). This calculation may show that the choice of a constant stress distribution is physically sound and confirms the importance of obtaining a tangible bridging effect in the very neighborhood of the crack tip. Such a mechanism is available in the WC/Co cermet since the metal phase continuously circumvents all the ceramic grains. Thus, although the ultimate strength of

the metal ligament may be lower than that of an individual ceramic crystallite, high toughness is achieved due to a more effective bridging stress distribution as compared to monolithic ceramics toughened through bridging of individual crystallites.

4 Conclusions

An experimental analysis of the toughening behavior of a WC/Co cermet material has been presented, which is based on both the assessment of rising *R*-curve behavior upon stable crack propagation and the experimental determination of COD profiles by SEM observations. According to the microscopy evidence of stretched Co ligaments shielding the crack along a limited extension of the order $\Delta a^* \approx= 100\,\mu$m, a near-tip crack bridging mechanism has been assumed as the main factor responsible for the toughening effect. A theoretical analysis using the mechanics of cracks bridged within a small process zone enabled us to explain the sharply rising *R*-curve behavior of the WC/Co cermet. For doing so, a bridging stress distribution was taken along the crack profile abscissa, x', both in the functional form, $\sigma_{BR}(x') = \alpha x'^2 - \beta x'^3$, or as a constant value. The constant stress distribution was found to lead to a more conceivable value of the ultimate strength of the metal ligaments as compared to the other proposed bridging stress distribution. The theoretical COD profile along the bridged crack, as calculated by using a constant $\sigma_{BR}(x')$ function), was found to reasonably fit the COD profile experimentally determined by SEM mapping. The present study was motivated by the intention of deeply understanding the excellent fracture behavior of the WC/Co cermet material and in order to apply the same toughening concept and microstructural approach to other cermet-type composites.

Acknowledgements

This work was perfomed during the stay of one of the authors (G.P.) at the Technical University Hamburg-Harburg (TUHH) under the support of the GKSS–TUHH grant for Micromechanics of Multiphase Materials.

References

1. Erdogan, Z. and Joseph, P. F., Toughening of ceramics through crack bridging by ductile particles. *J. Am. Ceram. Soc*., 1989, **72**, 262–270.
2. Rödel, J., Sindel, M., Dransmann, M., Steinbrech, R. W. and Claussen, N., *R*-curve behaviour in ceramic composites produced by directed metal oxidation. *Journal of the European Ceramic Society*, 1994, **14**, 153–161.
3. Thompson, L. R. and Raj, R., In situ stress–strain response of small metal particles embedded in a ceramic matrix. *Acta Metall. Mater*, 1994, **42**, 2477–2485.
4. Sigl, L. S. and Fischmeister, H. F., On the fracture toughness of cemented carbides. *Acta Metall*., 1998, **36**, 887–897.
5. Kotoul, M., On the shielding effect of a multiligament zone of a crack in WC/Co. *Acta Mater*., 1997, **45**, 3363–3376.
6. Pezzotti, G., Okamoto, Y., Nishida, T. and Sakai, M., On the near-tip toughening by crack-face bridging in particulate and platelet-reinforced ceramics. *Acta Mater*., 1996, **44**, 899–914.
7. Nojima, T. and Nakai, O., Stable crack extension of an alumina ceramic in three point bending test. *J. Soc. Mater. Sci. Jpn*, 1993, **42**, 412–418..
8. Nishida, T., Hanaki, Y. and Pezzotti, G., Effect of notch-root radius on the fracture toughness of fine-grained alumina ceramics. *J. Am. Ceram. Soc*., 1995, **77**, 606–608.
9. Nishida, T., Hanaki, Y., Nojima, T. and Pezzotti, G., Measurement of *R*-curve behavior in toughened silicon nitride by stable crack propagation in bending. *J. Am. Ceram. Soc*., 1996, **78**, 3113–3116.
10. Rödel, J., Kelly, J. F., Stoudt, M. R. and Bennison, S. J., A loading device for fracture testing of compact tension specimens in the scanning electron microscopes. *Scanning Micros*, 1991, **5**, 29–36.
11. Engel, U. and Huebner, H., Strength improvement of cemented carbides by hot isostatic pressing (HIP). *J. Mater. Sci*., 1978, **13**, 2003–2012.
12. Srawley, J. E. and Gross, B., *Cracks and Fracture*. American Society for the Testing of Materials Special Technical Publication no. 601, ed. J. L. Swedlow and M. L. Williams. American Society for Testing and Materials, Pittsburg, PA, 1976, p.559.
13. Irwin, G. R., In *Fracture*. Handbuch der Physik, Vol. 6. Springer–Verlag, Berlin, 1958.
14. Barenblatt, G. R., The mathematical theory of equilibrium cracks in brittle fracture. *Adv. Appl. Mech*., 1962, **7**, 55–129 .
15. Sih, G. C., *Handbook of Stress Intensity Factors*. Lehigh University Press, Bethlehem, PA, 1973.
16. Choi, S. R., Salem, J. A. and Sanders, W. A., Estimation of crack closure stresses for in situ toughened silicon nitride with 8 wt.% scandia. *J. Am. Ceram. Soc*., 1992, **75**, 1508–1511.
17. Pezzotti, G., Muraki, N., Maeda, N. and Nishida, T.*In situ* measurement of bridging stresses in toughened Si_3N_4 using Raman microprobe spectroscopy. *J. Am. Ceram. Soc*., in press.
18. Smithells, C. J., *Metals Reference Book*. Butterworths & Co., London, 1976.
19. Ashby, M. F., Blunt, F. J. and Bannister, M., Flow characteristics of highly constrained metal wires. *Acta Metall*, 1989, **37**, 1847–1857.